Particle & Particle Systems Characterization
www.particle-journal.com

Self-Organization of Anisotropic and Binary Colloids in Thermo-Switchable 1D Microconfinement

*Julius W. J. de Folter, Ping Liu, Lingxiang Jiang, Anke Kuijk, Henriëtte E. Bakker, Arnout Imhof, Alfons van Blaaderen, Jianbin Huang, Willem K. Kegel, Albert P. Philipse, and Andrei V. Petukhov**

Anisotropic and binary colloids self-assemble into a variety of novel supracolloidal structures within the thermo-switchable confinement of molecular microtubes, achieving structuring at multiple length scales and dimensionalities. The multistage self-assembly strategy involving hard colloidal particles and a soft supramolecular template is generic for colloids with different geometries and materials as well as their binary mixtures. The colloidal architectures can be controlled by colloid shape, size, and concentration. Colloidal cubes align in chains with face-to-face arrangement, whereas rod-like colloids predominantly self-organize in end-to-end configurations with their long axis parallel with the long axis of the microtubes. The 1D microconfinement imposed on binary mixtures of anisotropic and isotropic colloids further increases the diversity of colloid-in-tube structures. In cube–sphere mixtures, cubes may act as additional confiners, locking in colloidal sphere chains, while a "colloidal Morse code" is generated where rods and spheres alternate in the case of rod–sphere mixtures. The versatile confined colloidal superstructures including their thermoresponsive assembly and disassembly are relevant for the development of stimulus–responsive materials where controlled release and encapsulation are desired.

1. Introduction

The construction of self-assembled smart materials is rapidly developing by the design of new colloidal building blocks with increasingly complex geometries and tailored functionalities.[1] Hierarchical, bottom-up self-organization processes of nano- and microscale building blocks are widely encountered in nature[2] and constitute an important design route for stimulus-responsive materials. We recently introduced the hierarchical self-assembly of colloidal spheres inside molecular microtubes into a library of ordered structures, including double and triple helices.[3] Here, we demonstrate that a rich variety of novel supracolloidal structures emerge from the self-organization of various shape-anisotropic colloids and binary mixtures of isotropic and anisotropic colloids in 1D microconfinement. The versatility of our thermo-switchable self-assembly strategy is highlighted by the use of a broad variety of colloids with different geometries, materials, and sizes as well as their binary mixtures.

The engineering of anisotropic colloidal building blocks has taken a flight over the last decade, yielding a diverse colloidal toolbox that opens up new pathways for the fabrication of advanced functional materials.[1,4–9] The continuing sophistication of colloid complexity to direct hierarchical self-organization is not restricted to the design of colloid shape alone but also includes further functionalization by chemical anisotropy,[4] which provides site-specific interactions such as in Janus or surface-patterned particles. Alternatively, external electric[5] or magnetic fields,[6] or polymer-induced depletion interactions[7] may be applied to steer multistage self-assembly of anisotropic colloids. Here, we exploit the use of microconfinement, based on molecular self-assembly, as a directing agent for the self-organization of ordered structures from anisotropic building blocks. Assembly of anisotropic building blocks induced by 1D confinement was investigated previously at the molecular scale, where ellipsoidal C_{70} fullerenes[10] and cube-shaped $H_8Si_8O_{12}$[11] were encapsulated in carbon nanotubes, but is largely unexploited in colloidal systems.

Dr. J. W. J. de Folter,[+] P. Liu, Dr. L. Jiang, Prof. W. K. Kegel, Prof. A. P. Philipse, Dr. A. V. Petukhov
Van't Hoff Laboratory for Physical and Colloid Chemistry
Debye Institute for Nanomaterials Science
Utrecht University
Padualaan 8, 3584, CH, Utrecht
The Netherlands
E-mail: a.v.petukhov@uu.nl
Dr. L. Jiang, Prof. J. Huang
Beijing National Laboratory for Molecular Sciences
College of Chemistry and Molecular Engineering
Peking University
100871, Beijing, China
Dr. A. Kuijk, H. E. Bakker, Dr. A. Imhof, Prof. A. van Blaaderen
Soft Condensed Matter
Debye Institute for Nanomaterials Science
Utrecht University
Princetonplein 1, 3584, CC, Utrecht, The Netherlands
[+]Present address: Unilever R&D, Olivier van Noortlaan 120, 3133AT, Vlaardingen, The Netherlands.

DOI: 10.1002/ppsc.201400132

Self-assembly from mixtures of two distinct isotropic building blocks has yielded binary crystals, which can act as a model system for atomic crystals[12] or display interesting opto-electrical properties.[13] Self-organizing systems containing both anisotropic and isotropic building blocks have been investigated to some extent in bulk,[14] not in confinement. In this study, we additionally investigate the hierarchical assembly of binary mixtures from anisotropic and isotropic colloids in the confinement of molecular microtubes. Such intricate self-assembled structures may prove helpful in the development of novel technology for stimulus-responsive information-bearing materials.

2. Results and Discussion

2.1. Colloidal Cubes in 1D Microconfinement

The effects of molecular self-assembly and tubular confinement on the assembly of anisotropic building blocks were investigated employing cubic- and rod-like colloids. The hierarchical self-organization process of colloids in molecularly assembled microtubes is schematically outlined in **Figure 1**a for colloidal cubes. During the formation of the microtubes upon cooling isotropic mixtures containing 10 wt% sodium dodecyl sulfate (SDS) and β-cyclodextrin (β-CD) with a molar ratio of 1:2,[15] the colloids co-assemble within the ≈1 µm-sized microtube pores. Hematite cubes with edge lengths nearly matching the tube diameter form single particle chains within the cylindrical pores of the rigid microtubes (Figure 1b). To test whether the cubes form chains inside the microtubes owing to their magnetic nature, we additionally prepared nonmagnetic silica colloids with a cubic shape.[8] Since the size of the resulting colloids is tunable, we investigated the co-assembly of cubes with mean edge lengths d larger than, similar to, and smaller than the microtube diameter. Large cubes with edge lengths of 1.66 µm are excluded from the cylindrical microtube pores (see Figure 1c). These cubes are found outside the tubes as single particles and small clusters of particles with random

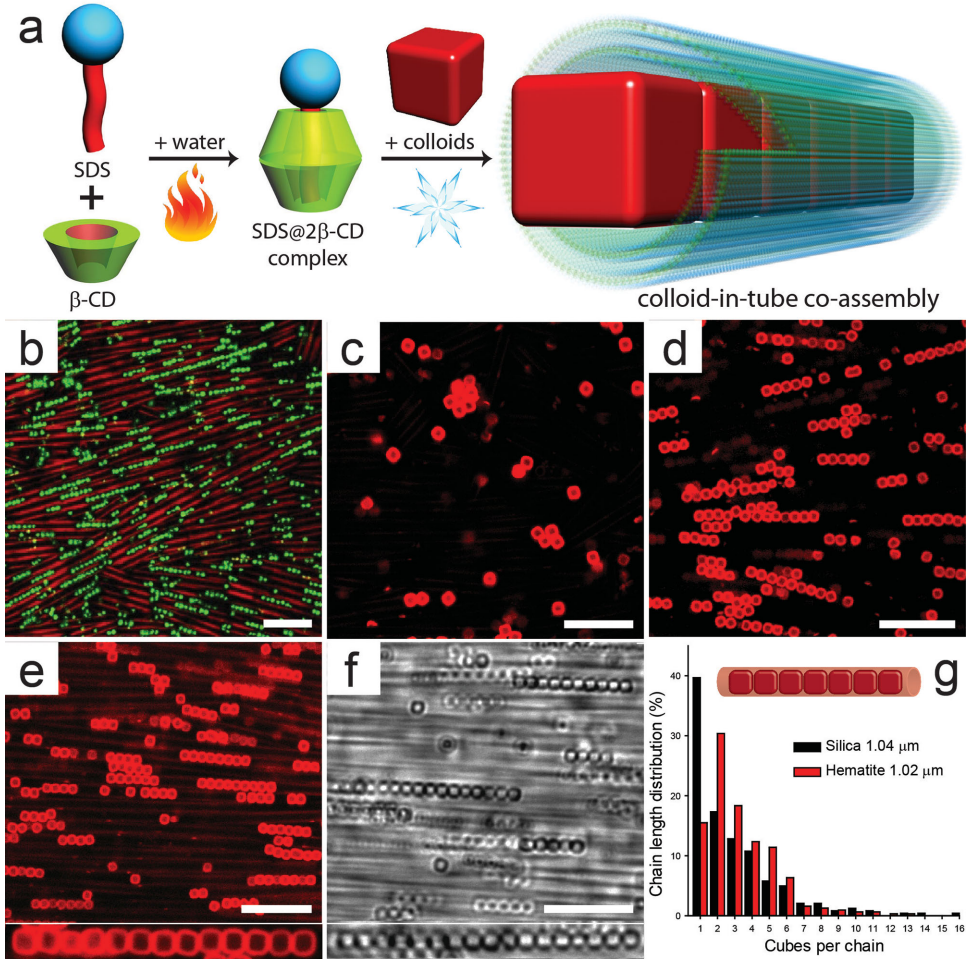

Figure 1. Size-dependent co-assembly of colloidal cubes and molecular microtubes. a) Schematic representation of the self-assembly of SDS/2β-CD (sodium dodecyl sulfate/β-cyclodextrin) inclusion complexes into microtubes, in which cubes arrange in chains. Self-organization of b) hematite and c–f) silica cubes in microtubes with cubic edge lengths d of, respectively, b) 1.02 µm (25 wt%); c) 1.66 µm (13 wt%); d) 1.30 µm (25 wt%); and e,f) 1.04 µm (25 wt%). Cubes with edge lengths close to the microtube pores assemble in chains with face-to-face arrangement (b,d,e); large cubes are excluded from the pores, are disordered and immobile (c), while small cubes form Brownian chains (Figure S1, Supporting Information). Laser scanning confocal microscopy (LSCM, b–e) and optical microscopy (OM, f) images are shown. g) Cubic chain length distribution determined from ≥250 chains for hematite and silica cubes, as shown in (b) and (e), respectively. Scale bars are 10 µm.

orientations and are immobilized by the rigid, space-filling tubular surroundings. Cubes with edge lengths nearly equaling the microtube diameter predominantly organize inside the microtubes (Figure 1d–f). Apparently, the microtubes can adjust their diameter locally, which enables them to accommodate cubes with edge lengths slightly larger than the average tube diameter. They display a striking preference for assembly in colloidal chains with the cubes favoring a face-to-face arrangement. Apart from chains of cubes, some singular particles are encountered as well. Once the microtubes have formed, the cubes are fixed and unable to move within the microtube network.

The 1D chains of face-to-face-aligned cubes have various lengths and may become longer than 20 cubes. The relative amount of chains monotonically decreases with chain length for nonmagnetic silica cubes (Figure 1g). However, in the case of hematite cubes the number of dimers and trimers exceeds the amount of single cubes, most probably due to their magnetic character. Since the edge length is the shortest axis of the cube, they fit most efficiently within the pores in a face-to-face alignment. For cubes with d = 1.04 μm (Figure 1e,f), very close to the tube diameter, reorientation is therefore nearly impossible. Moreover, it is likely that there are slight attractions, which favor the largest contact area between the cubes. Finally, the smallest cubes used in this study (d = 802 nm, see Figure S1, Supporting Information) also assemble into 1D colloidal chains. Due to their smaller size, the chains and single colloids retain their dynamic, Brownian character. Control over the supracolloidal cube structures was not only provided by cube size but was also demonstrated by the incorporation of different amounts of cubes. **Figure 2** shows that also the chain length distribution can be manipulated by varying the concentration of colloidal cubes. With increasing concentration, the amount of single cubes decreased and both the chain length and proportion of longer chains increased.

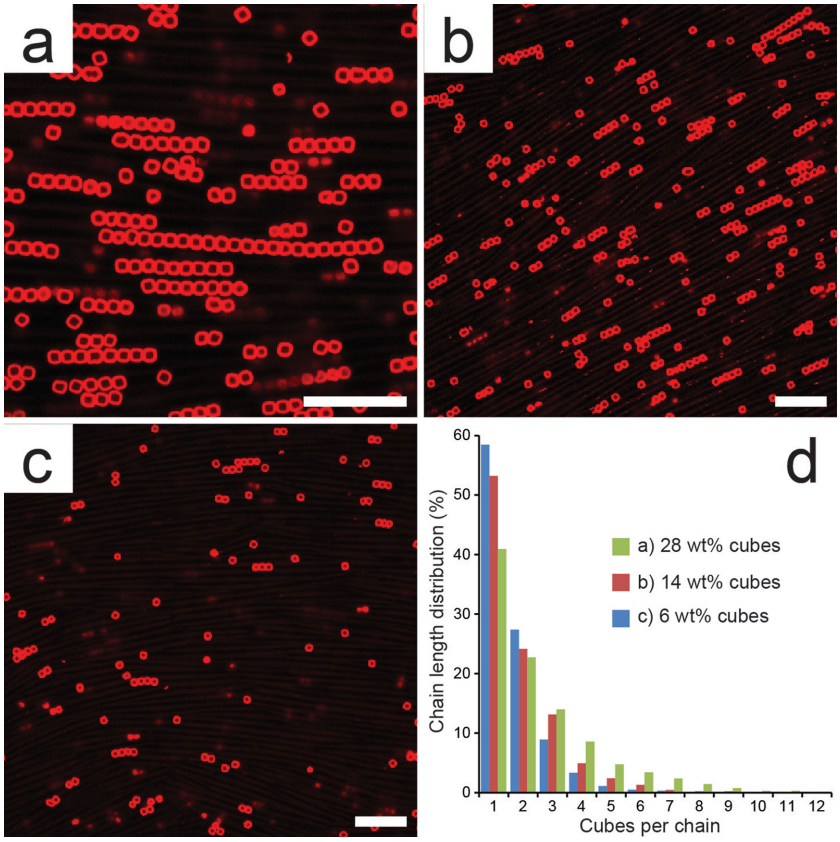

Figure 2. Control over chain length distribution by varying the concentration of colloidal cubes. LSCM images showing the co-assembly of colloidal cubes with cubic edge lengths of 1.04 μm and microtubes as tuned by the incorporation of a) 28 wt%, b) 14 wt%, and c) 6 wt% cubes, respectively. d) Corresponding cubic chain length distributions as determined from >500 chains. Scale bars are 10 μm.

2.2. Rod-Like Colloids in 1D Microconfinement

Furthermore, fluorescently labeled rod-like silica colloids[9] were mixed with SDS and β-CD to study their co-assembly with microtubes (**Figure 3**). Since the rods are longer and their widths are smaller than the tube diameter, the only way for them to be incorporated in the tubes is with their long axis parallel with the tube walls. This is demonstrated in Figure 3a–f for rods with three different sizes and aspect ratios. The majority of the rods organize in straight supracolloidal chains with an end-to-end configuration. Therefore, rods may act as directional tracers for the microtubes. Alternatively, since rods have some lateral freedom within the pores, they may increase their packing fraction by assembling in tilted chains (Figure 3d), where rods make an angle with the long axis of the microtubes. Alternatively, if rods are thin enough (Figure 3d,f), they can assemble in close-packed double chains with two particles side-by-side. Multiple configurations were encountered at a fixed rod concentration. For thicker rods, the cylindrical pores only allow for the incorporation of single particles (Figure 3e). The rods are not fixed in their position within the tubes, but they display distinctive 1D movements along the long axis of the tubes (see Supporting Information Videos S1 and S2). Due to geometrical restrictions, flipping of rods around their long axis was not observed regardless of their size. In addition, the length distribution of rod chains could be tuned by rod concentration as shown in Figure S2 (Supporting Information). With increasing colloid concentration, longer chains were encountered and the average chain length increased.

As another example of anisotropic colloids, we used peanut-shaped hematite particles with a magnetic character, further validating that the assembly of colloids is general with respect to both shape and material of the colloids. In addition to silica and polystyrene colloids,[3] aqueous hematite colloids with anisotropic shapes[16] also form self-organized structures. Similar to cubes (Figure 1b), hematite peanuts are found inside the microtubes, as displayed in Figure 3g. They are forced to align

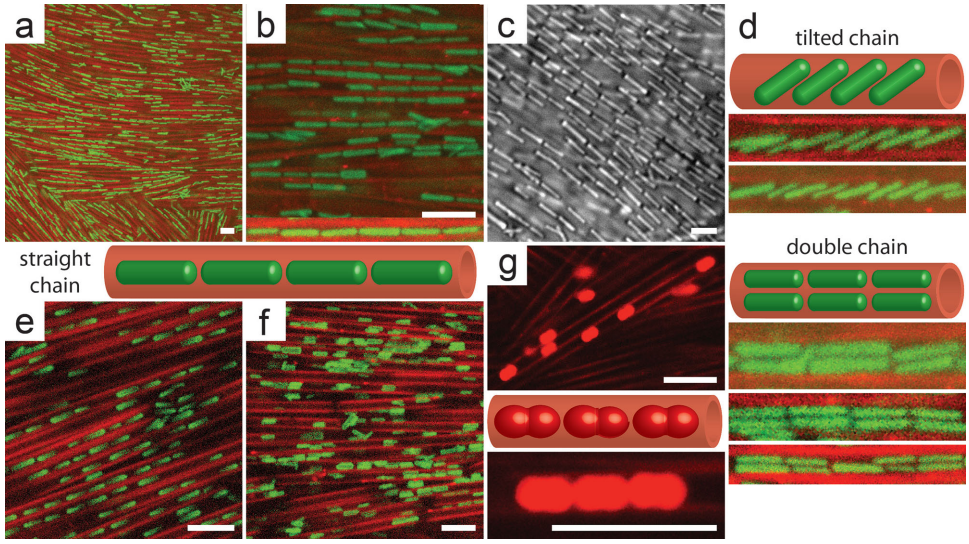

Figure 3. Confinement-induced self-organization of colloidal rods in microtubes. Silica rods with respective lengths of a–d) 2.86 × 0.51 μm (L/D = 5.8, 29 wt%); e) 2.30 × 0.60 μm (L/D = 3.8, Supporting Information Video S1, 15 wt%); and f) 1.80 × 0.40 μm (L/D = 4.5, Supporting Information Video S2, 12 wt%) assemble in colloidal chains. g) Co-assembly of hematite peanuts (1.72 × 0.70 μm, 12 wt%) and microtubes. Both rods and peanuts align with their long axis parallel with the long axis of the microtubes, while rods may also arrange in tilted and double chains (d). Scale bars are 5 μm.

their long axis with the tube direction, since only the short axis fits within the tube diameter. The magnetic dipole moment of the peanuts, however, is perpendicular to their long axis,[16d] so chains of peanut-shaped colloids with their preferred magnetic orientation cannot be formed in the micropores. Interestingly, application of a magnetic field did not significantly influence the colloidal structures due to the confining network of rigid microtubes. However, when the magnetic field was applied before microtube formation, larger colloidal structures formed that were not embedded in the microtubes.

2.3. Binary Colloid Mixtures in 1D Microconfinement

In a number of studies, the potential of self-assembled materials from mixtures of anisotropic and isotropic building blocks has been recognized,[14] but the effect of confinement was not investigated thus far. Therefore, we use binary mixtures of anisotropic and isotropic building blocks and investigate their assembly in cylindrical confinement, as shown in **Figure 4** for cube–sphere and rod–sphere mixtures. When both cubes and spheres are incorporated in microtubes, colloidal structures emerge where cubes and spheres alternate and display a rich variety of binary architectures (Figure 4a and Figure S3, Supporting Information). Since the cubes cannot move within the microtubes, the spheres may be trapped in a state of ultimate confinement as they not only experience the confinement of the microtube walls but also are additionally locked in by the immobilized cubes, which act as additional confiners. We identify a number of similarities and differences with respect to assembly of only one type of colloid. When a number of cubes form a chain without any spheres in between, they still prefer a face-to-face arrangement similar to assembly without spheres. As expected from the sphere size (D = 508 nm) with respect to tube diameter, sphere structures with zigzag and helical configurations are observed. However, cubes and spheres mutually influence the eventual structures they form. For instance, spheres can assemble side by side in the proximity of a cube and display a square-like arrangement, usually locked in between two cubes. This configuration is not encountered in the absence of cubes and can be related to a slight increase in pore size induced by the cubes as their edge lengths are slightly larger than the mean pore size. Additionally, cubes with a tilted orientation were also only observed in cube–sphere mixtures, not without spheres. Interestingly, whenever cubes are tilted at least one up till four spheres are located close to the faces of the cubes. In this way, the spheres force the cube to rotate and adopt a tilted orientation, thereby realizing a binary structure with a high packing efficiency. Despite the large diversity of supracolloidal binary structures within one sample, the colloid arrangements could be controlled to some extent by cube–sphere ratio and colloid concentration (see Figure S3, Supporting Information). Binary structures shifted from sphere- to cube-dominated with increasing cube–sphere ratio, although similar structural elements were encountered in all samples.

The co-assembly of rods and spheres, as shown in Figure 4b and Figure S4 (Supporting Information), generates a so-called colloidal Morse code, since a variety of binary colloidal structures are incorporated within the microtubes. Typically, spheres assemble in zigzag structures until a rod is encountered. The number of spheres between the rods varies. Rods either display a straight configuration, where the long axis of the rod aligns parallel with the long axis of the microtube, or a tilted configuration. Although rods cannot flip, they can act as a colloidal switch: straight and tilted configurations are interchangeable as the rod–sphere structures are subject to Brownian motion within the confinement of the cylinder. In other words, the spheres smoothly transmit their dynamic zigzag structure to the rods and determine the configuration of the rods. Since the sphere diameter matches the rod thickness,

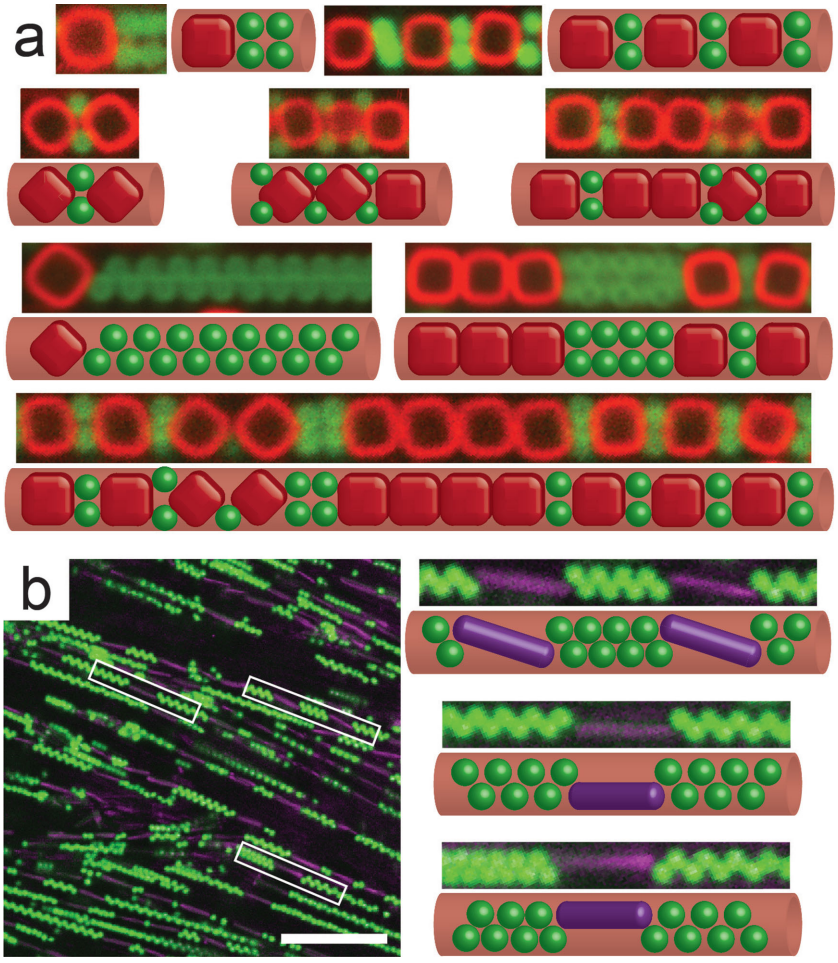

Figure 4. Colloid-in-tube co-assembly employing binary mixtures from anisotropic and isotropic colloids, demonstrated by LSCM images and accompanying sketches. a) Cylindrically confined cube–sphere mixtures (13 and 8.7 wt%, respectively) yield a variety of binary colloidal architectures. Cubes ($d = 1.04$ μm) do not move within the microtubes and act as additional confiners, locking in sphere structures (diameter $D = 508$ nm), see also Figure S3 (Supporting Information). b) Rod–sphere mixtures (24 and 11 wt%, respectively) confined in the microtubes generate a so-called colloidal Morse code, where colloidal rods with dimensions of 2.86×0.51 μm either display a straight or tilted orientation and alternate with zigzag structures from colloidal spheres ($D = 508$ nm), see also Figure S4 (Supporting Information). Scale bar is 10 μm.

the rod ends take a position at the ends of the zigzag sphere structure where logically, in the absence of rods, a sphere would be located.

2.4. Thermo-Switchability and Co-Assembly Mechanism

The colloid-in-tube co-assembly can also be controlled externally, as it is switchable with temperature (**Figure 5**, Supporting Information Videos S3–S5). Upon heating, the microtubes melt and the colloids are not confined within the microtubes anymore and move randomly throughout the sample in an isotropic state. The melting process is followed in time for cubes and rods in Figure 5a,d, respectively. The transition from the ordered to the isotropic state is especially clear for the rods, as it is marked by a randomization of the direction of the rods. Upon cooling, the microtubes and colloidal structures they enclose reassemble (Figure 5b,e). The final stages of chain assembly are characterized by fast 1D movements of colloids in the direction of the micropores, as shown in Figure 5c for cubes. Hence, the colloid-in-tube co-assembly is fully reversible with temperature, which may be valuable for controlled release and encapsulation applications. In addition, if a chemical reaction or another fixating step like use of an electric field and/or temperature[17] is used, the presented 1D structures could also be made permanent at elevated temperatures.

The whole set of data presented here and in our previous work[3] suggests that there is a mechanism promoting formation of close-packed structures. Colloidal particles are forced to enter the microtubes simply because there is very little space available outside the microtubes, which form a space-filling structure. The particle distribution inside each microtube can be considered inhomogeneous, where significant empty spaces and close-packed arrangements of colloids alternate. For example, helical structures formed by spheres[3] can be solely explained by the need to achieve the most efficient space filling.[18] In Figure 1, one observes only face-to-face configuration of cubes, which yield the closest-packed structure. However, addition of spheres, which can profit from the creation of additional pockets by turning the cubes by 45°, induce new configurations presented in Figure 4a. This result can again be understood by the tendency toward close-packed structures. Similar conclusions can be drawn by observing the structures formed by rods and their mixtures with spheres.

We have demonstrated that the tendency toward close-packed structures is generic and does not depend on the chemical nature of the particles and the details of their surface structure. Colloidal chains are absent in both the pure aqueous colloidal dispersions and at elevated temperatures in the presence of SDS and β-CD in the isotropic state and only start appearing during the formation of the microtubes. Some generic attraction between colloids can be induced by a depletion effect caused by (complexes of) SDS and β-CD molecules. Their influence could be enhanced in 1D structures since the entropy loss by the colloids attaching to a chain is smaller than in 3D. The kinetics and dynamics of the co-assembly process, involving both the microtube formation and the supracolloidal structure generation, very likely contribute to the inhomogeneous distribution of the particles between the microtubes. Further experimental and theoretical investigations are needed to clarify the exact mechanistic details of the multistage co-assembly process.

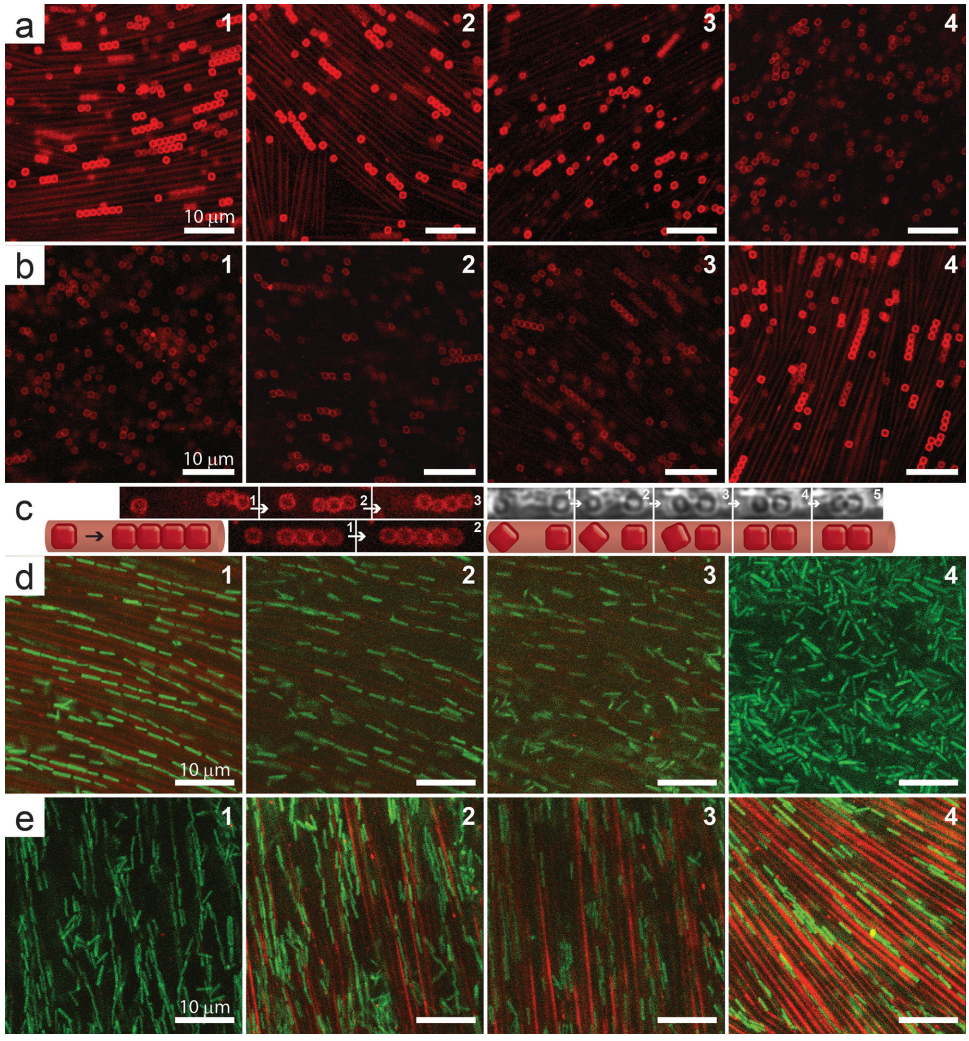

Figure 5. Thermo-reversibility of cube-in-tube and rod-in-tube co-assembly, as displayed by LSCM image sequences. a) Melting of SDS/β-CD microtubes and encapsulated colloidal cube chains (d = 1.04 µm, 15 wt%) with face-to-face arrangement at $T > 35$ °C and b) their restoration upon cooling (see Supporting Information Video S3). c) Colloidal chain formation from cubes during final stages of the cooling process. d) Disassembly of microtubes and the release of incorporated, aligned rod chains reaching an isotropic state with random orientations of rods (2.86 × 0.51 µm, 29 wt%) at elevated temperatures and e) their reassembly upon cooling. The complete process can be followed in Supporting Information Videos S4 and S5.

3. Conclusion

We have shown the hierarchical self-assembly of shape-anisotropic colloids and their binary mixtures with isotropic colloids in the confinement of molecular microtubes. The thermo-switchable co-assembly of cyclodextrin-surfactant microtubes and colloids is generic for colloids with different geometries, materials as well as binary colloid mixtures. Supracolloidal structures could be controlled by colloid shape, size, and concentration. Cubes predominantly align in chains with face-to-face arrangement, whereas rod-like colloids are unable to rotate freely and are forced to arrange with their long axis parallel with the long axis of the microtubes. In addition, we have introduced the self-organization of binary mixtures of anisotropic and isotropic colloids in confinement, further increasing the diversity of colloid-in-tube structures. In the co-assembly of cube–sphere mixtures, cubes may act as additional confiners, locking in colloidal sphere chains. When both rods and spheres are embedded in the micropores, a so-called switchable colloidal Morse code is generated where rods and spheres alternate. The microconfinement of supracolloidal structures including their thermoresponsive assembly and disassembly, all of which can be monitored in situ, are relevant for applications in controlled release and encapsulation. Moreover, the robustness of our multistage co-assembly approach involving the self-organization of supracolloidal architectures inside a soft supramolecular template, yielding structuring at multiple length scales, may prove much more versatile than the work presented here. Although the self-assembly mechanism has not been fully elucidated yet, the surprising versatility provides some insightful self-assembly design rules from which more controlled particle systems may evolve, so that stimulus-responsive and information-bearing materials can be developed. For instance, currently we are aiming to exploit our insights and gain additional control over the supracolloidal architectures generated by using other external stimuli apart from temperature

such as application of an external magnetic field to manipulate arrangements of incorporated magnetic spheres.

4. Experimental Section

Preparation of the Microtubes: To prepare a microtube stock suspension, SDS, beta-cyclodextrin (β-CD), and water were weighed into a 20-mL vessel to give a mixture with a total concentration of SDS and β-CD of 10 wt% and a molar ratio between SDS and β-CD of 1:2. The mixture was heated to ≈60 °C to obtain a transparent, isotropic solution, which was then cooled to room temperature to allow for the formation of microtubes.[15] The microtube suspension was viscous and turbid.

Colloids: The co-assembly of anisotropic colloids and binary colloid mixtures with β-CD/SDS microtubes was studied. RITC-dyed colloidal silica cubes[8] with various edge lengths (1.66 μm, 1.30 μm, 1.04 μm, and 802 nm) were used. Furthermore, FITC-dyed silica rods[9] with different dimensions (2.86 × 0.51 μm, 2.30 × 0.60 μm, and 1.80 × 0.40 μm) were employed. Additionally, the behavior of hematite cubes (edge length of 1.02 μm) and peanuts (1.72 × 0.70 μm) was studied.[16] Stöber silica spheres (diameter of 508 nm) were mixed with cubes or rods to study binary colloid mixtures in the cylindrical confinement of microtubes. The size polydispersity was ≤5% for the various colloidal dispersions studied and <10% for the silica rods, both in length and diameter.

Mixing Colloids with Microtubes: To prepare colloid-in-tube samples, known volumes of colloidal stock suspensions with known weight percentage of colloids were centrifuged at 2–3000 rpm for 15 min in centrifuge sample tubes. This was followed by removal of the supernatant water in the case of hematite dispersions or ethanol in the case of silica dispersions. The weight of the remaining colloids after evaporating water or ethanol was determined using an analytical weighing balance. Silica colloids were transferred from ethanol to water by at least two redispersion and centrifugation cycles. A known weight of microtube stock suspension (typically, 1 g) was added to the centrifuge tube to give a final mixture-containing colloids with concentrations of 2–30 wt%. Exact colloid concentrations for specific experiments can be found in the figure captions. The sample was heated to ≈60 °C to melt the microtubes and was sonicated to disperse the colloids. Then, the centrifuge tube was cooled to room temperature. Upon cooling, the sample was gently rotated to avoid sedimentation of the colloids.

Microscopy: Before imaging, microtube/colloid mixtures were usually placed in glass capillaries (Vitrocom, 0.1 × 2 × 50 mm), which were sealed by UV-curing epoxy glue. Samples that were imaged by laser scanning confocal microscopy (LSCM) were dyed by adding a solution of Nile Red in acetone (1 mg mL^{-1}) to the microtubes. Acetone evaporated upon heating of the sample. Samples were imaged with a Nikon TE 2000U laser scanning confocal microscope equipped with a Nikon C1 scanning head in combination with an Ar-ion laser (488 nm, Spectra Physics), a HeNe laser (543.5 nm, Melles Griot), and an oil immersion lens (100× Nikon Plan Apc, NA 1.4). In addition, samples were imaged with a Nikon inverse optical microscope equipped with an oil immersion 100× Nikon objective. Images were taken with a Lumenera InfinityX CCD camera. The thermal behavior of the samples was investigated using a Linkam THMS600 microscope heating stage.

Supporting Information

Supporting Information is available from the Wiley Online Library or from the author.

Acknowledgements

This work is financially supported by The Netherlands Organization for Scientific Research (NWO) and the National Natural Science Foundation of China (21273013 and 21073006). The authors thank Utrecht University for the short stay grant of L.J. and China Scholarship Council for the fellowship of P.L. The authors also thank Robin Geitenbeek and Sonja Castillo for particle synthesis.

Received: June 18, 2014
Revised: September 15, 2014
Published online: October 13, 2014

[1] a) S. C. Glotzer, M. J. Solomon, *Nat. Mater.* **2007**, *6*, 557; b) S. Sacanna, D. J. Pine, *Curr. Opin. Colloid Interface Sci.* **2011**, *16*, 96; c) K. Miszta, J. de Graaf, G. Bertoni, D. Dorfs, R. Brescia, S. Marras, L. Ceseracciu, R. Cingolani, R. van Roij, M. Dijkstra, L. Manna, *Nat. Mater.* **2011**, *10*, 872; d) P. F. Damasceno, M. Engel, S. C. Glotzer, *Science* **2012**, *337*, 453; e) T. Gibaud, E. Barry, M. J. Zakhary, M. Henglin, A. Ward, Y. Yang, C. Berciu, R. Oldenbourg, M. F. Hagan, D. Nicastro, R. B. Meyer, Z. Dogic, *Nature* **2012**, *481*, 348; f) S. Sacanna, M. Korpics, K. Rodriguez, L. Colon-Melendez, S. Kim, D. J. Pine, G. Yi, *Nat. Commun.* **2013**, *4*, 1688.

[2] G. M. Whitesides, B. Grzybowski, *Science* **2002**, *295*, 2418.

[3] L. Jiang, J. W. J. de Folter, J. Huang, A. P. Philipse, W. K. Kegel, A. V. Petukhov, *Angew. Chem Int. Ed.* **2013**, *52*, 3364.

[4] a) Q. Chen, J. K. Whitmer, S. Jiang, S. C. Bae, E. Luijten, S. Granick, *Science* **2011**, *331*, 199; b) Y. Wang, Y. Wang, D. R. Breed, V. N. Manoharan, L. Feng, A. D. Hollingsworth, M. Weck, D. J. Pine, *Nature* **2012**, *491*, 51; c) L. Feng, R. Dreyfus, R. Sha, N. C. Seeman, P. M. Chaikin, *Adv. Mater.* **2013**, *25*, 2779; d) S. H. Kim, A. D. Hollingsworth, S. Sacanna, S. J. Chang, G. Lee, D. J. Pine, G. R. Yi, *J. Am. Chem. Soc.* **2012**, *134*, 16115.

[5] a) N. Yanai, M. Sindoro, J. Yan, S. Granick, *J. Am. Chem. Soc.* **2012**, *135*, 34; b) F. Ma, S. Wang, L. Smith, N. Wu, *Adv. Funct. Mater.* **2012**, *22*, 4334.

[6] a) D. Zerrouki, J. Baudry, D. Pine, P. Chaikin, J. Bibette, *Nature* **2008**, *455*, 380; b) J. Yan, M. Bloom, S. C. Bae, E. Luijten, S. Granick, *Nature* **2012**, *491*, 578; c) S. Sacanna, L. Rossi, D. J. Pine, *J. Am. Chem. Soc.* **2012**, *134*, 6112; d) J. Yan, K. Chaudhary, S. C. Bae, J. A. Lewis, S. Granick, *Nat. Commun.* **2013**, *4*, 1516.

[7] a) S. Sacanna, W. T. M. Irvine, P. M. Chaikin, D. J. Pine, *Nature* **2010**, *464*, 575; b) D. J. Kraft, R. Ni, F. Smallenburg, M. Hermes, K. Yoon, D. A. Weitz, A. van Blaaderen, J. Groenewold, M. Dijkstra, W. K. Kegel, *Proc. Natl. Acad. Sci. USA* **2012**, *109*, 10787; c) K. Zhao, T. G. Mason, *Phys. Rev. Lett.* **2007**, *99*, 268301.

[8] L. Rossi, S. Sacanna, W. T. M. Irvine, P. M. Chaikin, D. J. Pine, A. P. Philipse, *Soft Matter* **2011**, *7*, 4139.

[9] a) A. Kuijk, A. van Blaaderen, A. Imhof, *J. Am. Chem. Soc.* **2011**, *133*, 2346; b) A. Kuijk, A. Imhof, M. H. W. Verkuijlen, T. H. Besseling, E. R. H. van Eck, A. van Blaaderen, *Part. Part. Syst. Charact.* **2014**, *31*, 706.

[10] A. N. Khlobystov, R. Scipioni, D. Nguyen-Manh, D. A. Britz, D. G. Pettifor, G. A. D. Briggs, S. G. Lyapin, A. Ardavan, R. J. Nicholas, *Appl. Phys. Lett.* **2004**, *84*, 792.

[11] J. Wang, M. K. Kuimova, M. Poliakoff, G. A. D. Briggs, A. N. Khlobystov, *Angew. Chem Int. Ed.* **2006**, *45*, 5188.

[12] M. E. Leunissen, C. G. Christova, A. P. Hynninen, C. P. Royall, A. I. Campbell, A. Imhof, M. Dijkstra, R. van Roij, A. van Blaaderen, *Nature* **2005**, *437*, 235.

[13] E. V. Shevchenko, D. V. Talapin, N. A. Kotov, S. O'Brien, C. B. Murray, *Nature* **2006**, *439*, 55.

[14] a) M. Adams, Z. Dogic, S. L. Keller, S. Fraden, *Nature* **1998**, *393*, 349; b) G. H. Koenderink, G. A. Vliegenthart, S. G. J. M. Kluijtmans, A. van Blaaderen, A. P. Philipse, H. N. W. Lekkerkerker, *Langmuir* **1999**, *15*, 4693; c) G. A. Vliegenthart, H. N. W. Lekkerkerker, *J. Chem. Phys.* **1999**, *111*, 4153; d) D. Kleshchanok, A. V. Petukhov, P. Holmqvist, D. V. Byelov, H. N. W. Lekkerkerker, *Langmuir*

2010, *26*, 13614; e) D. Kleshchanok, J. M. Meijer, A. V. Petukhov, G. Portale, H. N. W. Lekkerkerker, *Soft Matter* **2012**, *8*, 191.
[15] L. X. Jiang, Y. Peng, Y. Yan, M. L. Deng, Y. L. Wang, J. B. Huang, *Soft Matter* **2010**, *6*, 1731.
[16] a) J. W. J. de Folter, E. M. Hutter, S. I. R. Castillo, K. E. Klop, A. P. Philipse, W. K. Kegel, *Langmuir* **2014**, *30*, 955; b) T. Sugimoto, K. Sakata, *J. Colloid Interface Sci.* **1992**, *152*, 587; c) T. Sugimoto, M. M. Khan, A. Muramatsu, *Colloids Surf., A* **1993**, *70*, 167; d) S. H. Lee, C. M. Liddell, *Small* **2009**, *5*, 1957.
[17] a) H. R. Vutukuri, J. Stiefelhagen, T. Vissers, A. Imhof, A. van Blaaderen, *Adv. Mater.* **2012**, *24*, 412; b) H. R. Vutukuri, A. F. Demirörs, B. Peng, P. D. J. van Oostrum, A. Imhof, A. van Blaaderen, *Angew. Chem Int. Ed.* **2012**, *51*, 11249.
[18] G. T. Pickett, M. Gross, H. Okuyama, *Phys. Rev. Lett.* **2000**, *85*, 3652.